http://www.e-journals.net

ISSN: 0973-4945; CODEN ECJHAO
E-Journal of Chemistry
2011, **8(S1),** S225-S236

Rapid Determination of Aesculin, Aesculetin and Fraxetin in *Cortex Fraxini* Extract Solutions Based on Ultraviolet Spectroscopy

MING YANG*, JIA-LEI CHEN, XIU-FENG SHI and HUI-JUE NIU

Medicament Department
Longhua Hospital Affiliated to Shanghai Univesity of TCM Shanghai, China
yangpluszhu@sina.com

Received 24 May 2011; Accepted 16 July 2011

Abstract: To evaluate the application of ultraviolet spectroscopy for the rapid determination of aesculin, aesculetin and fraxetin in *Cortex fraxini* extract solutions, ultraviolet spectra of *Cortex fraxini* extract solutions from different batches were collected in the spectral range from 200 nm to 400 nm. The relationship between ultraviolet spectra and chemical parameters displayed some non-linear characteristics. Thus, K-OPLS was proposed to establish the calibration models for the determination of *Cortex fraxini* extract solutions between the reference data and ultraviolet spectra. The calibration results were achieved for the determination of *Cortex fraxini* extract solutions. The coefficients of determination in calibration (R^2) for aesculin, aesculetin and fraxetin were 0.989, 0.957 and 0.939, while in prediction (R^2) were 0.982, 0.979 and 0.962, respectively. And the root-mean-square error of prediction (RMSEP) for aesculin, aesculet and fraxetin were 11.99, 3.02 and 1.59 μg/mL. The results demonstrated that ultraviolet spectroscopy could be used for the rapid determination of these three components in *Cortex fraxini* extract solutions.

Keywords: Aesculin, Aesculetin, Fraxetin, Ultraviolet spectroscopy,

Introduction

The traditional herb and their preparations continue to grow in popularity for their medical use. Quality control for herbal products is essential. It includes many aspects such as identity, purity, content, other chemical, physical or biological properties and manufacturing process. The approach of quality control for herbal products is much more complex compared with synthetic products, since their manufacturing process contains much more stages such as harvest, drying, extraction and purification. Therefore, high quality products need

continuous process control and improvement. Process analytical technology (PAT)[1] is a revolution in the pharmaceutical industry initiated by the united states food and drug administration, which can be introduced to the herb manufacturing industry to reduce the risk of making a poor quality product. The key to practice PAT is to develop the process analyzers or process analytical chemistry tools[2]. Rapid analysis of the intermediates can consistently ensure a predefined quality at the end of the manufacturing process. Quantitative spectroscopic analysis is a rapid, easy-to-use and inexpensive analytical technique compared with chromatography determination. Although near infrared (NIR) spectroscopy is widely used to predict the chemical composition in the pharmaceutical industry[3,4], rapid analysis for process control is not limited to NIR[1] but can include many other spectroscopic analyses, such as Raman and ultraviolet (UV) spectroscopy. UV spectroscopy can be used for measurement when systems contain conjugated double bonds. Some papers[5-7] showed the potential of UV spectroscopy for rapid analysis of process control.

Typically, a chemometric problem can be defined as a relationship between chemical parameters and spectra data for quantitative spectroscopic analysis. There are many methods to establish the chemometric model. Partial least square (PLS) regression is currently the standard method in supervised linear modeling in the field of chemometrics. However, in many cases the relationship between chemical parameters and spectra data displays non-linear characteristics. Recently, the "kernel trick" has been efficient to deal with non-linear problems. Kernel-based orthogonal projections to latent structures (K-OPLS)[8,9] is a method that has the capacity to improve predictive performance considerably in situations where strong non-linear relationship exists.

In china, *Cortex fraxini* is mostly used in resisting inflammation, antivirus and so on. It contains three main coumarins which are aesculin, aesculetin and fraxetin. These three coumarins have conjugated double bonds and show strong UV activity. The contents of these coumarins decide the quality of *Cortex fraxini* extract solutions. As for *Cortex fraxini*, several papers[10-12] have reported analysis methods established by chromatography. However, these methods are time-consuming, expensive to perform and sample throughput is limited. No relevant reports were found involving the use of UV spectroscopy for simultaneous-determination of these three coumarins. The aim of this paper is to explore the feasibility of UV spectroscopy rapidly to determine these three coumarins by K-OPLS and provide a method for process quality control of *cortex fraxini* extract.

Experimental

Eleven batches of *Cortex fraxini* samples were collected from different geographical origins of china. Seven batches were from Shanxi province of china, two were from Liaoning province, one was from Anhui province and the remaining was from Hebei province.

Reagents and chemicals

Aesculin, aesculetin and fraxetin were purchased from china's national institute for the control of pharmaceutical and biological product. All organic solvents were HPLC grade. Orthophosphoric acid (H_3PO_4) was analytical grade (Lingfeng chemical co., Shanghai).

Apparatus and software

The high performance liquid chromatography (HPLC) system used was a Shimadzu CLASS-VP System equipped with a model series LC-10 ADVP Pump, FCV-10ALVP Low pressure gradient flow controller valve, SCL-10 ADVP controller, 20 μL loop injector, CTO-10As column oven and a SPD-M10AVP diode array detector. Data acquisition was performed on class-VP software.

A Shimadzu UV-2450 spectrophotometer equipped with a 1 cm quartz cell was used to measure absorbance. Data acquisition was performed on UV-Probe software. A SB2200 ultrasonic instrument (Bi Neng Xin ultrasonic instrument co. Shanghai, China) was used to extract *Cortex fraxini* samples.

The Robust Calibration toolbox, K-OPLS package and Statistic toolbox of Matlab 7.1 software were used for the statistical treatment of the data and application of various multivariate methods.

Sample preparation

Cortex fraxini extract solutions were obtained by ultrasonic method. Each powdered sample (4.0 g) was placed in the Erlenmeyer flask and was extracted with 100 mL distilled water. The first sample was collected after 30 minutes and then the sampling time lag was 10 minutes until the extraction extended 80 minutes. Each extract was filtered. For spectroscopy analysis, the solution was transferred accurately 0.1 mL to a 10 mL volumetric flask and distilled water was added to volume. For reference analysis, the solution was further filtered through 0.45 μm membrane filters. There were 6 samples in each batch and 66 samples in all.

Reference analysis

High performance liquid chromatographic method was developed for the determination of aesculin, aesculetin and fraxetin in *Cortex fraxini* extract solutions as reference. Compounds were separated on a 250 mm × 4.6 mm i.d., 5 μm particle, Kromasil RP C18 column protected by a guard column of the same type. A freshly prepared 13:87v/v mixture of methanol (component A) and water–phosphoric acid 99.9:0.1(v/v) (component B) was used as the mobile phase[13,14]. The flow rate of the mobile phase was maintained at 1 mL/min. The detection was carried out at 340 nm.

The amounts of the active compounds were determined by use of calibration plots established by chromatography of aesculin, aesculetin and fraxetin standards at five different injection contents. The corresponding peak areas were plotted against the contents of the compounds. Peaks were identified by comparison of retention times and UV absorption spectra against those of standards.

Spectral measurements

The UV spectra of samples was recorded over 200-400 nm wavelengths and absorbance was sampled at 0.5 nm intervals at room temperature with distilled water as reference.

Sample outliers analysis

In order to reduce the number of variables, principal component analysis (PCA) was performed. The samples were in a new reduction k-dimensional space (k<n). The mahalanobis square distance from the k factor score was calculated, which measured the distance of each observation from the center of the data in the new *k*-dimensional space. It was defined by the following equation:

$$D_i^2(t_i,\bar{t}) = (t_i - \bar{t})' S^{-1} (t_i - \bar{t}) > ACR \tag{1}$$

Where D_i^2 is the mahalanobis square distance, t_i is the score vector of *i*th sample, t is the centroid of the dataset, which is a *k*-dimensional vector with the means of each factor score as components, S represents the scores covariance matrix, ACR[15] denotes the critical value for the maximum squared mahalanobis distance. It was defined as follows:

$$ACR = \frac{k*(n-1)^2 * F_{k,n-k-1}}{n*(n-k-1)+n*k*F_{k,n-k-1}} \tag{2}$$

Where n is the number of observation, k is the number of factor, $F_{k,n-k-1}$ denotes F-distribution critical value with k and $n-k-1$ degrees of freedom using the Bonferroni correction. An observation with a large D_i^2 which is greater than the value of ACR can be considered as an outlier.

Calibration and prediction subset partitioning

The method, termed SPXY[16] (sample set partitioning based on joint x-y distances) was used for the calibration and prediction subset partitioning after the outliers had been removed. SPXY extends the Kennard-Stone (KS) algorithm by encompassing both independent variable (x) and dependent variable (y) differences in the calculation of inter-sample distances. According to SPXY, a normalized xy distance was calculated as

$$d_{xy}(p,q) = \frac{d_x(p,q)}{\max_{p,q\in[1,N]} d_x(p,q)} + \frac{d_y(p,q)}{\max_{p,q\in[1,N]} d_y(p,q)} \tag{3}$$

Where $d_{x(p,\ q)}$ denotes the Euclidean distances between the x-vectors of each pair (p, q) of samples, and $d_{y(p,\ q)}$ denotes the Euclidean distances between the y-vectors of each pair (p, q) of samples.

The selection started by taking the largest $d_{xy(p,\ q)}$. At each subsequent iteration, the algorithm selected the sample that exhibited the largest minimum distance with respect to any sample already selected. Such the procedure was repeated until the number of samples was achieved. In this work, the percentage of samples was 85% and 15% for the calibration and prediction sets after the outliers had been removed.

K-OPLS for calibration

Spectra data was rearranged in terms of the kernel gram matrix K, with entries $k_{i,j} = \kappa(x_i, y_j)$. In this study, the Gaussian kernel function was used as

$$K_{i,j} = \exp\left(\frac{-\|x-y\|^2}{2\sigma^2}\right) \tag{4}$$

Where σ is the parameter for the kernel function. Then the kernel matrices K were centered to model estimation. The K-OPLS algorithm modeled the kernel matrices K by means of a set of predictive components and a set of Y-orthogonal components. Thus, the predictive score matrix and the Y-orthogonal score vector were estimated. Subsequent to the estimation step of each Y-orthogonal component, the kernel matrices K were deflated by the Y-orthogonal variation, followed by a subsequent updating of the predictive score matrix and estimation of further Y-orthogonal components if required. The regression coefficients between the predictive score and the Y-score were estimated for prediction as follows[8,9].

$$\hat{Y} = T_{Pte}^{A_o+1} B_t C_p^T \tag{5}$$

$$B_t = (T_{Ptr}^{A_o+1^T} T_{Ptr}^{A_o+1})^{-1} T_{Ptr}^{A_o+1^T} U_p \tag{6}$$

Where A_o denotes the number of Y-orthogonal components, U_p is Y-score matrix, T_{ptr} and T_{pte} denotes the predictive training score and test score, respectively, B_t denotes the matrix with the U_p-T_p regression coefficients.

The kernel function parameter (σ) and the number of *Y*-orthogonal components (A_o) of the K-OPLS model were optimized by 10-fold cross-validation. Thus, a 10-fold cross-validation was performed: the spectra data samples in the calibration set were randomly partitioned into 10 equally sized folds. Subsequently, 10 iterations of calibration and validation were performed such that within each iteration a different fold of the data was held out for validation while the remaining 9 folds were used for calibration.

Results and Discussion

HPLC method

Figure 1 shows a typical HPLC chromatogram of *Cortex fraxini* extract solutions, which shows the good separation of aesculin, aesculetin and fraxetin from the other constituents. Table 1 shows the methodology parameters and the calibration curves of the HPLC method. The correlation coefficients were found to be higher than 0.9995. Relative standard deviation (RSD) of the repeatability (n=6) and intermediate precision (inter-day, n=6) of the peak areas of three components were found to be lower than 2.99% and 2.66%, respectively, which showed acceptable repeatability and precision. The good recovery values obtained suggested that the accuracy of the method was acceptable. The results indicate that the reference values obtained by this method are accurate and can be used in UV spectroscopy calibration.

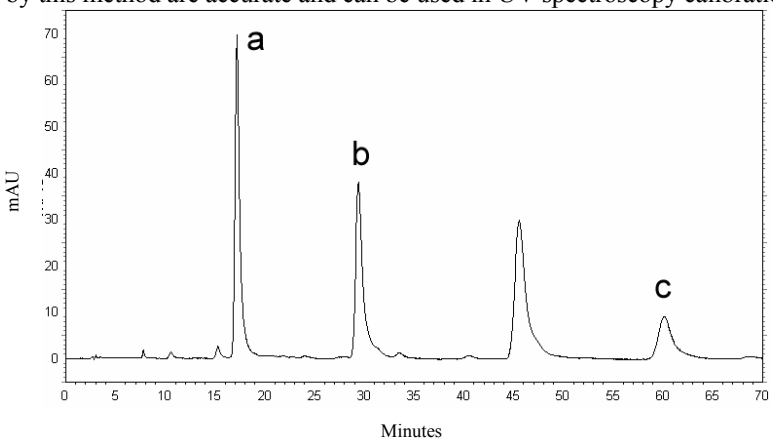

Figure. 1. HPLC chromatogram at optimized conditions (the peaks marked with a-c were aesculin, aesculetin and fraxetin)

Table 1. The methodology parameters and the calibration curve of the reference method

Compounds	Retention Time, min	Calibration curves	R	Test ranges, μg/ml	Linearity range, μg	Precision (RSD %, n=6)	Repeatability (RSD %, n=6)	Recovery, % n=6)
Aesculin	16.82	y=1959017x+ 196034	0.9995	126.0-551.7	1.20-6.00	0.62%	0.54%	103.41%
Aesculetin	29.02	y=3555568x+ 86920	0.9997	6.4-79.3	0.31-1.53	2.66%	2.99%	100.97%
Fraxetin	59.12	y=2795901x+ 29341	0.9999	4.1-33.8	0.10-0.52	0.48%	0.64%	101.66%

y: the peak area of chromatogram; x: the content of each compound

Spectroscopy measurement

Spectra of 66 samples were collected and are shown in Figure 2. The main features of the spectra are absorption bands at 202 nm, 286 nm and 337 nm, which are associated with those of the mixture of aesculin, aesculetin and fraxetin methanol solutions in our study. As expected, the similarity between the spectra was confirmed. Figure 3 shows the correlation coefficients between absorbance at each wavelength and the reference concentration of the samples. All the wavelengths are highly correlated ($|r| > 0.5$) with aesculin concentration, while wavelength regions show low correlation with aesculetin and show no correlation ($|r| < 0.5$) with fraxetin.

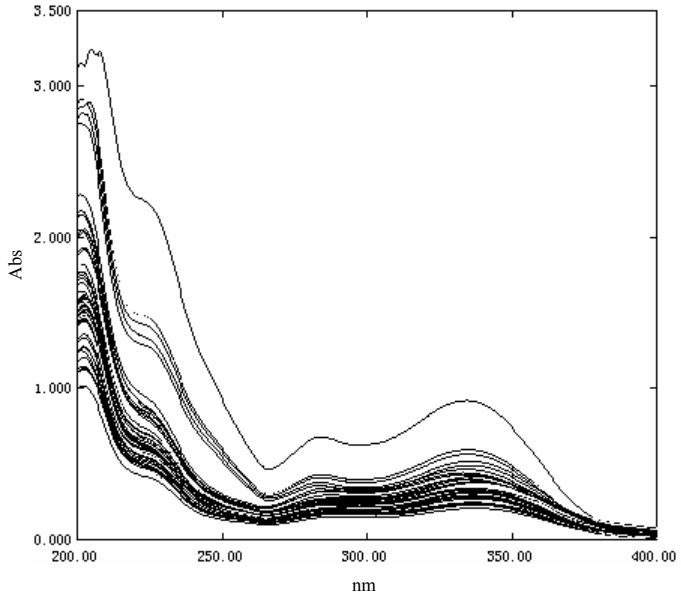

Figure 2. The UV spectra of the extract solutions of *Cortex fraxini*

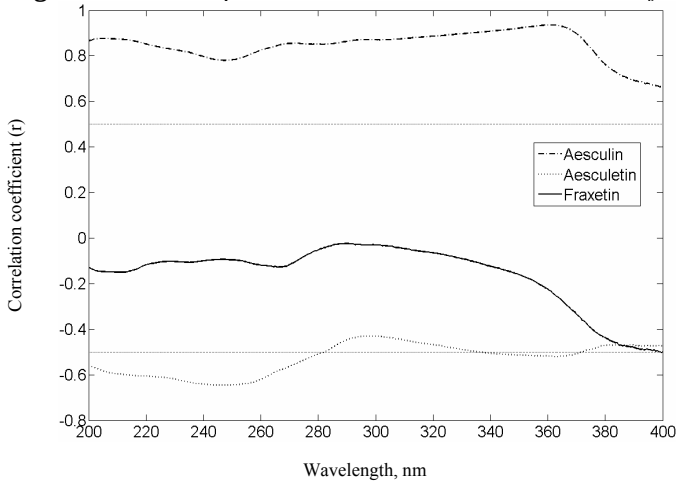

Figure 3. Correlation coefficients between absorbance at each wavelength and the reference concentration of the samples

Outliers detection and sample sets partition

After principal component analysis, the first two principal components had large variances and the cumulative proportion of the total sample variance was larger than 90%. Thus, the samples were in the new reduction 2-dimensional space for the outliers detection analysis. The histogram in Figure 4 shows the squared Mahalanobis distance values of samples in the new dimensional space. Consequently, only one sample's squared Mahalanobis distance value breaks through the ACR value line, which means the spectra of this sample is most unlike the spectra of the others. Therefore, this sample was considered as the outlier. After the outlier removal, there were 65 samples for sample sets partition. Table 2 shows the results after SPXY was performed. The ranges of the concentration of components in calibration set cover that in prediction set, which is helpful to build the robust calibration models.

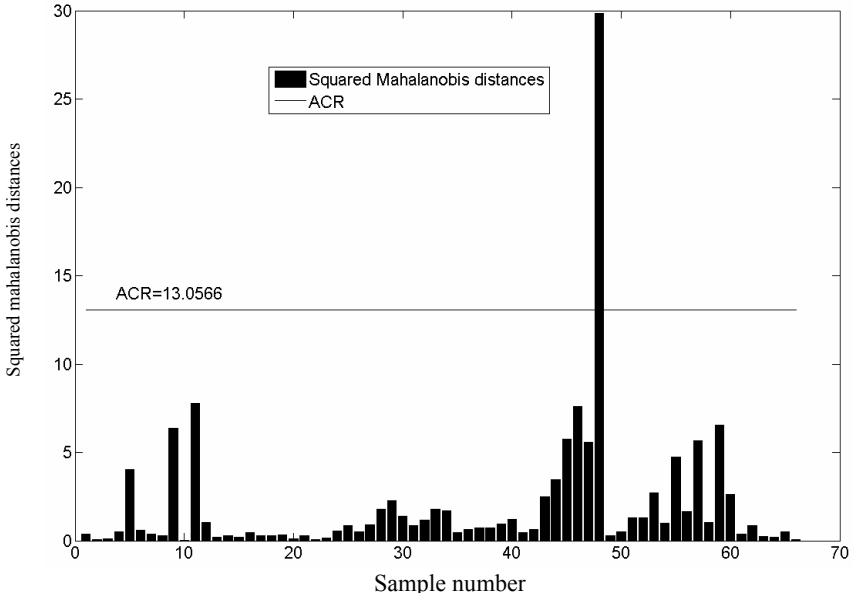

Figure 4. The squared mahalanobis distance values of samples and the ARC value (black line)

Table 2. Calibration and prediction subset partitioning after SPXY

Compounds	Calibration (n=55)		prediction (n=10)	
	Range, μg/mL	SD, μg/mL	Range, μg/mL	SD, μg/mL
Aesculin	126.00~551.70	112.56	236.50~476.70	86.88
Aesculetin	6.40~79.30	19.89	15.90~77.20	21.24
Fraxetin	4.10~33.80	6.63	4.80~27.10	7.95

SD: standard deviation

Calibration of K-OPLS models

Calibration set was used to build models and prediction set was used to test the robustness of the models. In this work, K-OPLS was performed with the Gaussian Kernel function. σ and A_o were optimized by 10-fold cross-validation, root mean square error of cross-validation (RMSECV) was calculated for each combination of σ and A_o parameters. These parameters were optimized by generating models with values of σ in the range of 1-50 and A_o in the

range of 1-20. Figure 5 shows the results after cross validation was performed. RMSECV is lowest when σ equals to 22 and A_o equals to 10 for aesculin, 31 and 9 for aesculetin, 10 and 12 for fraxetin. These optimum parameters were selected to model for these three components, respectively. RMSEC, RMSEP and corresponding coefficients of determination (R^2) were used for evaluating the calibration models. Table 3 shows the RMSEC, RMSEP and R^2 for all the calibration models of these three components. The coefficients of determination for calibration and prediction are all above 0.93, which suggest highly predictive and general models.

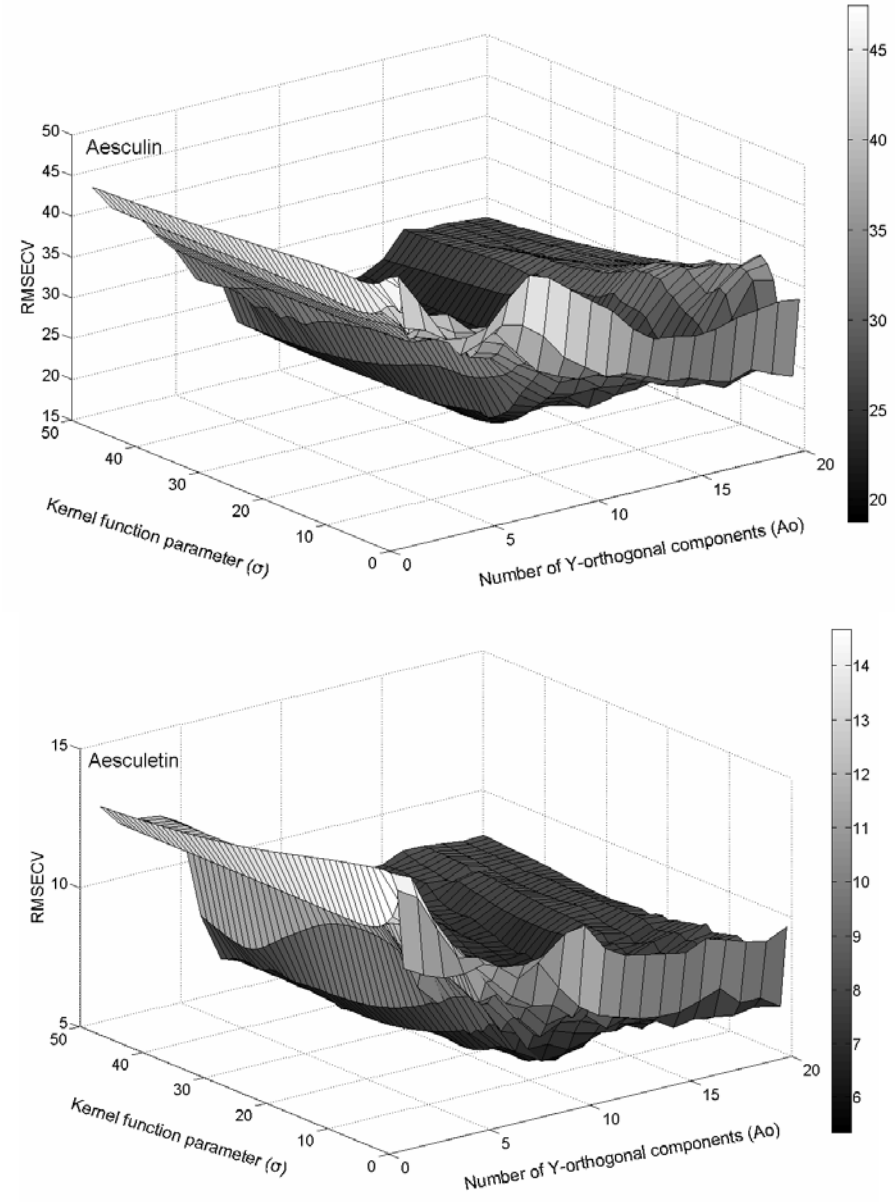

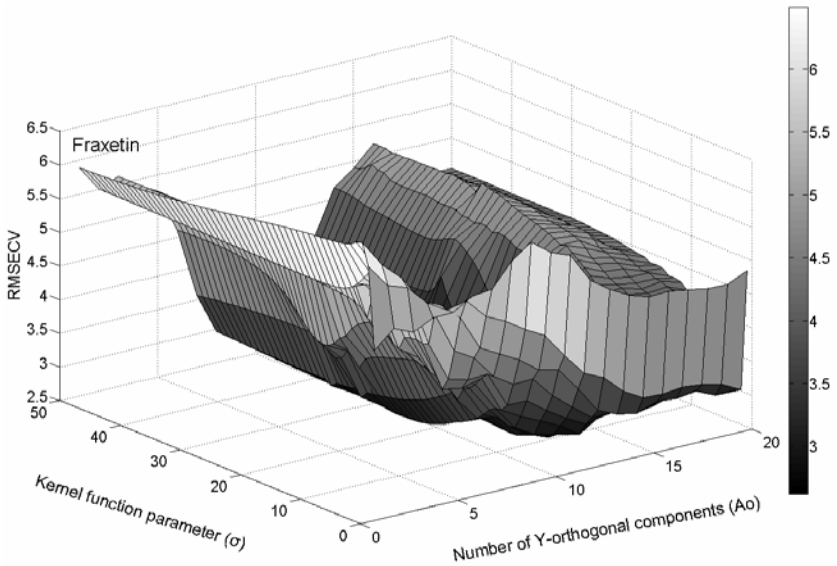

Figure. 5. RMSECV produced of each combination of σ and A_o parameters after cross validation

Table 3. The results of calibration and prediction of K-OPLS models

Components	σ	A_o	Calibration		Validation	Prediction	
			R^2	RMSEC, μg/mL	RMSECV, μg/mL	R^2	RMSEP, μg/mL
Aesculin	22	10	0.9892	11.59	18.76	0.9819	11.99
Aesculetin	31	9	0.9572	4.08	5.35	0.9789	3.02
Fraxetin	10	12	0.9392	1.62	2.62	0.9620	1.59

Figure 6 shows the correlations between the predicted concentration values and the reference values of the whole sample set of *Cortex fraxini* extract solutions after outlier removal. All of them show high correlations, which demonstrate that the established models can be used to predict the concentration of the three components in *Cortex fraxini* extract solutions.

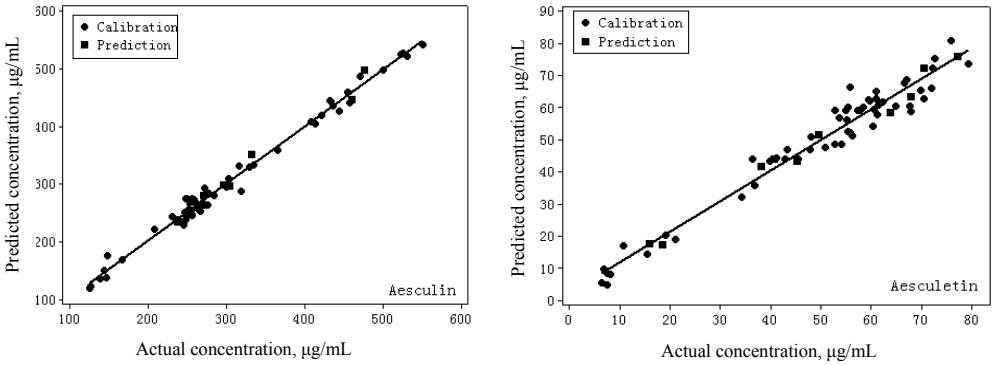

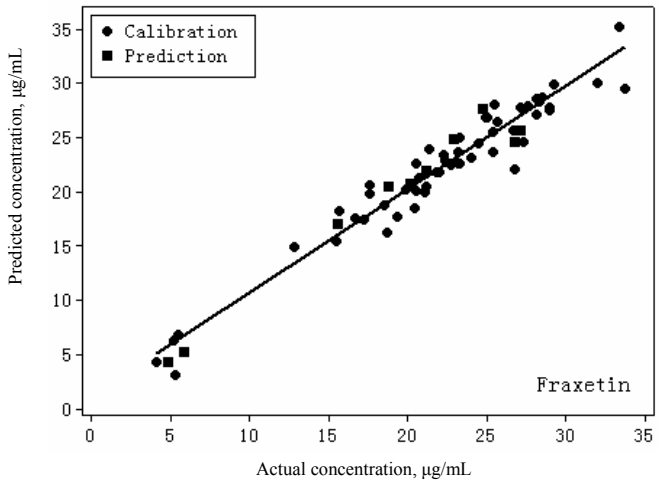

Figure 6. Correlation diagrams between the predicted values and the reference values of concentrations

Comparison with the results obtained by PLS

In parallel, PLS models were performed to model the spectra data and the concentration of components with 6, 7 and 6 latent variables as recommended by 10-fold cross-validation, respectively. Table 4 shows the RMSEC, RMSECV, RMSEP and R^2 for all the calibration models. The performance of the PLS calibration models for all the components were not as good as that of K-OPLS. Reasonable correlations, but poor accuracy were found for the predictions of aesculin (RMSEP=27.80 μg/mL) and aesculetin (RMSEP=6.74 μg/mL). The performance of fraxetin model was the worst, with the R^2 values lower than 0.62, which might be due to the low or non linear correlation between spectra absorbance and the concentration of the samples.

Table 4. The results of calibration and prediction of PLS model

Components	Latent variables	Calibration		Validation	Prediction	
		R^2	RMSEC, μg/ml	RMSECV, μg/mL	R^2	RMSEP, μg/mL
Aesculin	6	0.9388	27.60	25.86	0.8979	27.80
Aesculetin	7	0.9013	6.19	7.75	0.8935	6.74
Fraxetin	6	0.5815	4.25	4.00	0.6143	4.85

Application of the models for the analysis of unknowns

Six samples at different sampling points of different batches were collected. Then, the developed calibration models were used to predict concentration of these three components, and the HPLC method was also performed. The results are shown in Table 5. Most relative errors were less than 10% comparing the results of HPLC.

Table 5. The results of the models for the analysis of unknowns

S No	Aesculin			Aesculetin			Fraxetin		
	HPLC, μg/mL	Prediction, μg/mL	Relative errors, %	HPLC, μg/mL	Prediction, μg/mL	Relative errors, %	HPLC, μg/mL	Prediction, μg/mL	Relative errors, %
1	288.20	271.72	-5.72	69.70	70.79	1.56	27.80	26.69	-3.99
2	255.00	266.23	4.40	41.00	41.26	0.64	18.30	20.07	9.69
3	262.50	277.64	5.77	55.90	60.16	7.61	22.20	23.03	3.74
4	306.30	302.16	-1.35	54.40	51.15	-5.98	21.70	19.73	-9.06
5	285.40	284.94	-0.16	69.30	72.16	4.13	27.10	26.71	-1.45
6	271.90	281.95	3.70	62.80	69.57	10.79	25.10	25.08	-0.06

Conclusion

In this work, an UV spectroscopy method with K-OPLS as chemometric method was developed for the rapid determination of three coumarins in *Cortex fraxini* extract solutions. The performance of K-OPLS models were better than that of PLS models, which demonstrates that this chemometric method has the capacity to improve predictive performance considerably in situations where low or non linear correlation exits between spectra absorbance and the concentration of the samples. The results obtained showed that it was possible to determine the three coumarins in *Cortex fraxini* extract solutions with the proposed method.

Acknowledgment

The authors gratefully acknowledge the nature science foundation of Shanghai university of TCM, No. 09034. We are grateful to the website http://kopls.sourceforge.net/download.shtml, where we downloaded K-OPLS package freely and the website http://www.mathworks.com/matlabcentral/fileexchange/loadFile.do? objectId=12252, where we downloaded the outlier detection codes freely.

References

1. Shrestha B, Basnett H, Raj P M, Patel S S, Das M and Verma N K, *Res J Pharm Tech.,* 2009, **2(2),** 225-227.
2. Workman J, Koch M and Veltkamp D, *Process Anal Chem Anal Chem.*, 2007, **79(12),** 4345-4363.
3. Li W and Qu H, *J Pharm Biomed Anal.,* 2010, **52(4),** 425-431.
4. Li W, Xing L, Fang L, Wang J and Qu H, *J Pharm Biomed Anal*., 2010, **53(3),** 350-358.
5. Yin C, Shen Y, Liu S, Yin Q, Guo W and Pan Z, *Computers and Chemistry*, 2001, **25(3),** 239-243.
6. Zhao M B, Jiang Y, Zhang H Q and Tu P F, *China J Chin Mat Med.,* 2008, **33(7)**, 769-771, 821.
7. Di Nezio Pistonesi M S, Centurión M F, Palomeque M E, Lista A G and Fernández Band B S, *J Brazilian Chem Soc.,* 2007, **18(7),**1439-1442.
8. Rantalainen M, Bylesjö M, Cloarec O, Nicholson J K and Holmes E, *J Trygg J Chemometrics,* 2007, **21(7-9),** 376-385.
9. Bylesjo M, Rantalainen M, Nicholson J K, Holmes E, *J Trygg BMC Bioinformatics*, 2008, **9**, 106.
10. Liu L M, Chen L, Wang R H, Yang Q, Weng X G and Wang L, *China J Chin Mat Med.,* 2008, **33(24),** 2932-2935.

11. Zhou L, Kang J, Fan L, Ma X C, Zhao H Y, Han J, Wang B R and Guo D A, *J Pharm Biomed Anal*,.,2008, **47(1),** 39-46.
12. Li C, Chen A, Chen X, Ma X and Hu Z, *Biomed Chromatogr.*, 2005, **19(9),** 696-702.
13. Yang M, Yu M Y, Shi X F and Teng Y P, *China J Chin Mat Med.,* 2008, **33(22),** 2622-2626.
14. Yang M, Zhou Y, Chen J, Yu M, Shi X and Gu X, *China J Chin Mat Med.,* 2009, **34(20),** 2594-2598.
15. Trujillo-Ortiz A, Hernandez-Walls R, Castro-Perez A and Barba-Rojo K, A MATLAB file [WWW document]. (2006), URL http://www. mathworks.com/ matlabcentral/fileexchange/loadFile.do?objectId=12161.
16. Galvão R K H, Araujo M C U, José G E, Pontes M J C, Silva E C and Saldanha T C A, *Talanta*, 2005, **67(4),** 736-740